EXPERIMENTAL STUDY ON IGNITION CHARACTERISTIC AND PERFORMANCE OF A TWO-STROKE ENGINE FUELED WITH AVIATION KEROSENE

Zhiqiang Han[1,2,3], Xuantao Li[4], Wei Tian[1,2,3], Jia Fang[1,2,3], Xueshun Wu[1,2,3], Zinong Zuo[1,2,3,*], Yi Wu[1,2,3], Yan Yan[1,2,3]

[*1] Key Laboratory of Fluid and Power Machinery, Ministry of Education, Xihua U niversity, Chengdu 610039, China

[2] Key Laboratory of Fluid Machinery and Engineering, Sichuan Province, Xihua University, Chengdu 610039, China

[3] Engineering Research Center of Intelligent Space Ground Integration Vehicle and Control, Ministry of Education, Xihua University, Chengdu 610039, China

[4]School of Automobile and Transportation, Xihua University, Chengdu 610039, China

[*] Corresponding author; E-mail: zuozinong@mail.xhu.edu.cn (Zinong Zuo)

Abstract*: Two-stroke spark ignition engines are widely used in Unmanned Aerial Vehicles. Aviation kerosene offers advantages over aviation gasoline due to its higher flash point and lower volatility, making it likely to be adopted more widely in the future. However, the poor evaporation and atomization characteristics of aviation kerosene result in suboptimal ignition performance, especially in the engine start-up phase. To explore the fitting mixture concentration and temperature conditions for achieving better ignition performance of aviation kerosene, A series of experimental studies are conducted on a two-stroke engine. The intrinsic factors affecting engine performance are analyzed. The experimental results indicate that optimal ignition characteristics, maximum power output, and a reduced misfire rate can be achieved at mixture concentration of 0.6 and mixture temperature of 80°C. Furthermore, the misfire rate is most sensitive to the combustion duration, while the cyclic variations show significant sensitivity to ignition delay. The results provide guidance for optimizing ignition performance during the start-up phase of two-stroke engines fueled with aviation kerosene.*

Keywords : Two-stroke spark ignition engine; Unmanned Aerial Vehicles; Aviation kerosene; Experimental study; Ignition characteristics

1. Introduction

Two-stroke spark ignition (SI) engines have been widely used in the field of Unmanned Aerial Vehicles (UAVs) due to their high power-to-weight ratio and simplicity in operation and maintenance [1]. Although UAVs originated in the military sector, they are now flourishing in the civilian market as well [2-4]. The low ignition point and high volatility of aviation gasoline restrict its storage, transportation, and safety, prompting researchers to explore the more stable and safer option of aviation kerosene [5]. Compared to aviation gasoline, it has a similar low heating value and theoretical air-fuel ratio, along with a faster combustion velocity in the latter half of the combustion process [6]. This leads to lower fuel consumption and emissions [7], which makes it an ideal alternative fuel to aviation gasoline [8-10]. However, due to the low saturated vapor pressure of 5.4 kPa (at 38°C) and its higher kinematic viscosity, the formation of a homogeneous mixture is hindered [11]. Additionally, its overall combustion time is 21.2% longer than that of aviation gasoline [12]. Consequently, the start-up phases of the two-stroke engine encounter challenges such as ignition difficulties, prolonged ignition times, and instability [13].

To address the aforementioned issues, the significant attention has been garnered for research into the ignition characteristics of aviation kerosene combustion. To enhance the accuracy and reliability of simulations for the aviation kerosene combustion process, many researchers have focused on developing efficient chemical reaction kinetic models. Elliott et al. [14] highlighted the crucial role of these models in achieving accurate combustion process simulations. Yu et al. [15] created models that effectively predict the ignition, oxidation, and flame propagation mechanisms of RP-3 aviation kerosene. Mao et al. [16] explored the ignition behavior of RP-3 aviation kerosene across various temperatures using their combustion chemical kinetic model. They found that the Negative Temperature Coefficient of ignition delay time first decreases and then increases as the temperature rises. Yang et al. [17] and Meng et al. [18] conducted in-depth studies on RP-3 aviation kerosene. The latter even proposed a micro-explosion calculation equation, indicating that RP-3 exhibited relative stability during combustion without significant fluctuations. The above studies have made significant progress in modeling chemical reaction kinetics and combustion mechanisms. However, those models often have limited applicability and require simplifications in their calculations. Additionally, they do not adequately address the combustion process under specific operating conditions in two-stroke engines.

Some researchers have focused on experimental investigations of the ignition characteristics of aviation kerosene. Liu et al. [19] discovered through visualization studies that the ignition delay time of RP-3 decreases as the initial temperature rises, while laminar combustion velocity slows down when the temperature drops. Wang et al. [20] found through constant-volume combustion tests that the combustion time decreases initially and then increases as the mixture concentration (λ) of aviation kerosene rises. Chen et al. [21] discovered through simulation analysis that a two-stroke aviation kerosene engine can achieve better combustion ignition performance by using a rich air-fuel mixture. Du et al. [22] also found that through constant-volume combustion tests. When using aviation kerosene, different injection volume corresponds to different injection pressure, which can make it have

better ignition performance. The aforementioned studies provide valuable data for parameters such as ignition delay time and combustion speed of aviation kerosene. However, these studies primarily focus on static conditions and lack an in-depth analysis of combustion ignition characteristics under dynamic operating conditions in two-stroke engines.

To address those shortcomings, some researchers have conducted studies using actual engines. Chang et al. [23] discovered that the atomization of non-direct injection aviation kerosene fuel was inadequate, making engine start-up challenging without external assistance. Li et al. [24] concluded that the start-up ignition performance of two-stroke engines can be enhanced by increasing ignition energy without the need for additional auxiliary ignition systems. Zhang et al. [25] found that when the excess air coefficient is within the range of 0.6-0.8, the engine can start quickly and smoothly, with minimal fluctuations in cylinder pressure. Liang et al. [26] found that CO_2 exhibits a suppressive effect on the ignition of RP-3 aviation kerosene when the cylinder temperature is below 1300 K. Javed et al. [27, 28] found that aviation kerosene with good atomization characteristics can reduce ignition delay time and the minimum ignition temperature. Existing research has provided extensive data and theoretical analysis on the ignition characteristics and start-up performance of aviation kerosene. However, there remains a lack of systematic studies on the effects of λ and mixture temperature (T) on ignition characteristics during the start-up phase.

During actual engine operation, the λ and T in the cylinder continuously change on a single cycle scale. The ignition phenomenon is often the result of accumulated conditions over multiple cycles, making the ignition process more complex and difficult to predict. This study utilizes a two-stroke engine start-up performance testing platform. A systematic analysis is conducted on how the λ and T influence the ignition characteristics and engine performance during the start-up phase. Ignition characteristic parameters are investigated as cylinder pressure, heat release rate, peak in-cylinder temperature, ignition delay, center of combustion and combustion duration. The engine performance parameters are investigated as brake power, misfire rate, and cycle variations. In order to explore the relationship between the ignition characteristic parameters on the performance stability, they were analyzed using multiple linear regression method. The results of this study are helpful for optimizing the ignition control strategy of a two-stroke engine fueled by aviation kerosene.

2. Experimental methods

2.1. Experiment instrumentation and fuel

This study focuses on a 10 kW horizontally opposed SI two-stroke engine, model FQ170, with its main parameters presented in Tab. 1. To fulfill the testing requirements for transient data acquisition and analysis. A start-up performance testing platform for the two-stroke engine is established. The test platform comprises three systems, which includes the engine system, electronic control unit (ECU) system, and signal acquisition system. The structure of the engine start-up test platform, along with its components, is illustrated in Fig. 1 and 2. An air heater is positioned at the front end of the engine intake tract to warm the intake air. An air flowmeter is installed before the throttle to measure airflow. A photoelectric encoder (POSITAL (720P/R) IXARC) is attached to one end of the engine shaft to monitor

the crankshaft position. A cylinder pressure sensor (KISTLER 6054BR) linked to a charge amplifier (KISTLER 5011B) and a PT1000 temperature sensor are mounted on the engine head to measure instantaneous cylinder pressure and temperature. A wide-area oxygen sensor is installed on the exhaust pipe and connected to an exhaust λ analyzer (HORIBA MEXA-730λ). All sensor signals are connected to the host computer via the NI data acquisition card (NI USB-6343). The ECU is used to control the throttle opening and manage fuel injection and ignition based on crankshaft position.

Tab. 1. Engine parameters

Engine specification	parameters
Type of engine	Two-stroke, spark-ignition engine
Bore (mm)	52
Stroke (mm)	40.3
Displacement (mL)	170
Compression ratio	6.7
Rated power (kW)/(rpm)	10/7200
Rated torque (N·m)/(rpm)	14/6000
Ignition advance angle (°CA before the top dead center (BTDC))	30

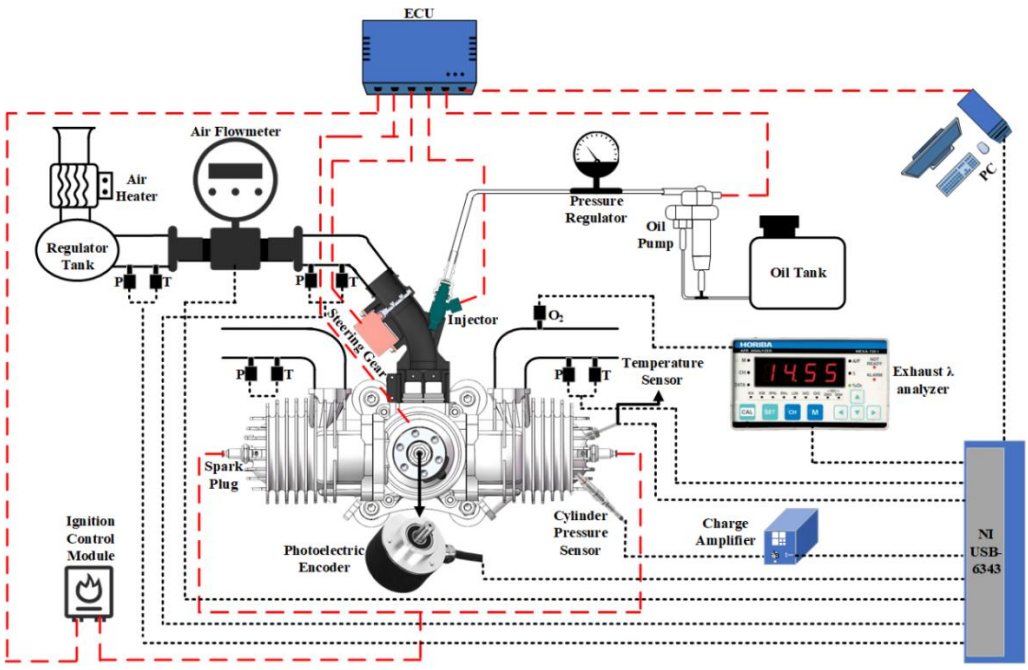

Fig. 1. Schematic diagram of test system

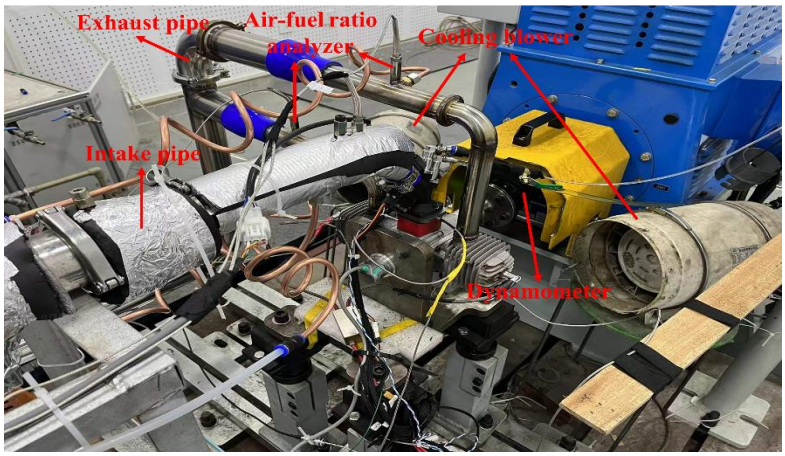

Fig. 2. Engine start-up and ignition test platform

The aviation kerosene used in the experiment is RP-3, and the fuel characteristics are compared with those of aviation gasoline in Tab. 2 below.

Tab. 2. Comparison of characteristics between RP-3 and aviation gasoline.

Fuel characteristics	RP-3	Aviation gasoline
Carbon Number	C_7–C_{16}	C_5–C_{11}
Density at 20 ℃ (kg/m^3)	775–830	700–750
Kinematic viscosity at 20 ℃ (mm^2/s)	1.25	0.8
Low heat value (MJ/kg)	43.4	43
Octane number	48	92
Cetane number	42	-
Saturated vapor pressure at 38 ℃ (kPa)	5.4	57.5–88
Flash point (K)	311	-45–-25
Stoichiometric air-to-fuel ratio	14.65	14.8

2.2. Experiment procedure and parameters definition

The test is conducted by controlling the engine intake temperature to regulate the T. To minimize magnetic interference from the dynamometer, a thermistor temperature sensor is mounted 5 cm in front of the engine air intake. Prior to the test, the dynamometer is used to operate the engine in reverse at low speed. The engine's internal flow path is heated by high-temperature air to match the intake air temperature, preventing heat loss of the mixture in the intake tract and crankcase. Once the engine temperature stabilizes, the engine is quickly towed back to the set start-up speed, followed by data collection. This study employs the excess air coefficient to characterize λ. The excess air coefficient is defined as the ratio of the actual air-fuel supply to the theoretical air volume, reflecting the adequacy of air-fuel mixing

during combustion. The λ is calculated based on the intake flow rate and injection pulse width, as shown in Eq. (1). The results are further validated using an exhaust λ analyzer.

$$\lambda = \frac{m_{\text{air}}}{m_{fuel}\lambda_0} \tag{1}$$

Where, m_{air} is the mass of air drawn into the cylinder per cycle; m_{fuel} is the amount of fuel supplied per cycle; λ_0 is the theoretical mass of air required for complete combustion of a unit mass of fuel. This paper investigates the engine start-up phase, which is difficult for fuel evaporation and requires the actual mixture concentration to be greater than the theoretical mixture concentration. As a result, the interval of λ=0.5-0.9 is selected for the study.

Ignition delay (θ_{ID}) is defined as the crankshaft rotation angle experienced from the start of spark plug ignition until the accumulated heat release reaches 10%. Center of combustion (θ_{CC}) is defined as the crankshaft angle corresponding to a cumulative heat release of 50%. Combustion duration (θ_{CD}) is defined as the crankshaft rotation angle experienced by the cumulative heat release from 10% to 90%. The heat release rate (*HRR*) is calculated as shown in Eq. (2).

$$\frac{dQ}{d\theta} = \frac{k}{k-1}p\frac{dV}{d\theta} + \frac{k}{k-1}V\frac{dp}{d\theta} \tag{2}$$

Where, k is specific heat ratio; p is cylinder pressure; V is instantaneous cylinder volume; and θ is instantaneous crank angle. The cumulative heat release is then obtained by integrating the *HRR*, which is calculated as shown in Eq. (3).

$$Q(\theta) = \int_{\theta_0}^{\theta} \frac{dQ}{d\theta} \tag{3}$$

Where, θ_0 is the starting crank angle of the initial integral.

The engine cyclic variations are expressed by the parameter COV_{IMEP}, which is calculated as shown in Eq. (4) [29].

$$COV_{IMEP} = \frac{\sigma_{IMEP}}{\overline{IMEP}} \times 100\% \tag{4}$$

Where, σ_{IMEP} is the standard deviation of 100 cycles of indicated mean effective pressure (IMEP), and $\overline{IMEP}$ is the mean of 100 cycles of IMEP.

3. Results and Discussion

3.1. Ignition characteristic

3.1.1 Cylinder pressure and heat release rate

The experiment collected data from 100 cycles under the following conditions. The engine speed (n) n=2000 rpm, throttle opening (TP) TP=25%, T=70-100 °C, and λ=0.5-0.9. Fig. 3 illustrates the impact of λ and T on cylinder pressure and heat release rate as the

crankshaft angle varies. As λ gradually increases, the peak cylinder pressure (P_{max}) initially increases and then decreases in Fig.3(a). Similarly, the peak of *HRR* (HRR_{max}) follows the same trend. Moreover, the crankshaft angle corresponding to their peaks exhibits an initial advance followed by a delay. When λ=0.9, both P_{max} and HRR_{max} experience a significant drop compared to other concentrations. This can be attributed to the poor evaporation and atomization performance of aviation kerosene. Under the same atomization temperature conditions, a lower λ results in a higher probability of large fuel droplet aggregation. This makes it more difficult to form a proper mixture, resulting in slower flame propagation and longer combustion duration. Conversely, the amount of fuel participating in combustion decreases, aside from the atomization effects with a larger λ. This result leads to the significantly reducing both P_{max} and HRR_{max} in poor combustion conditions.

As seen in Fig. 3(b), (c), and (d), with the increase in *T*, both P_{max} and HRR_{max} show a trend of initially increasing and then decreasing, with the corresponding crankshaft angle also exhibiting an initial advance followed by a delay. However, compared to Fig. 3(a), both P_{max} and HRR_{max} are larger, and there is a difference in the critical points of their trends. When T≥80 °C, it is evident that both the maximum P_{max} and maximum HRR_{max} shift toward smaller λ. At this point, the increase in *T* significantly enhances fuel evaporation and atomization, as well as increases the reaction rate. A smaller λ results in more fuel participating in the combustion reactions, which is leading to higher peak values and more concentrated heat release during combustion. However, *T* is a double-edged sword. It can significantly reduce intake flow, potentially leading to an unstable combustion process. Therefore, under the same λ conditions, both P_{max} and HRR_{max} demonstrate a trend of initially increasing and then decreasing when the *T* rises.

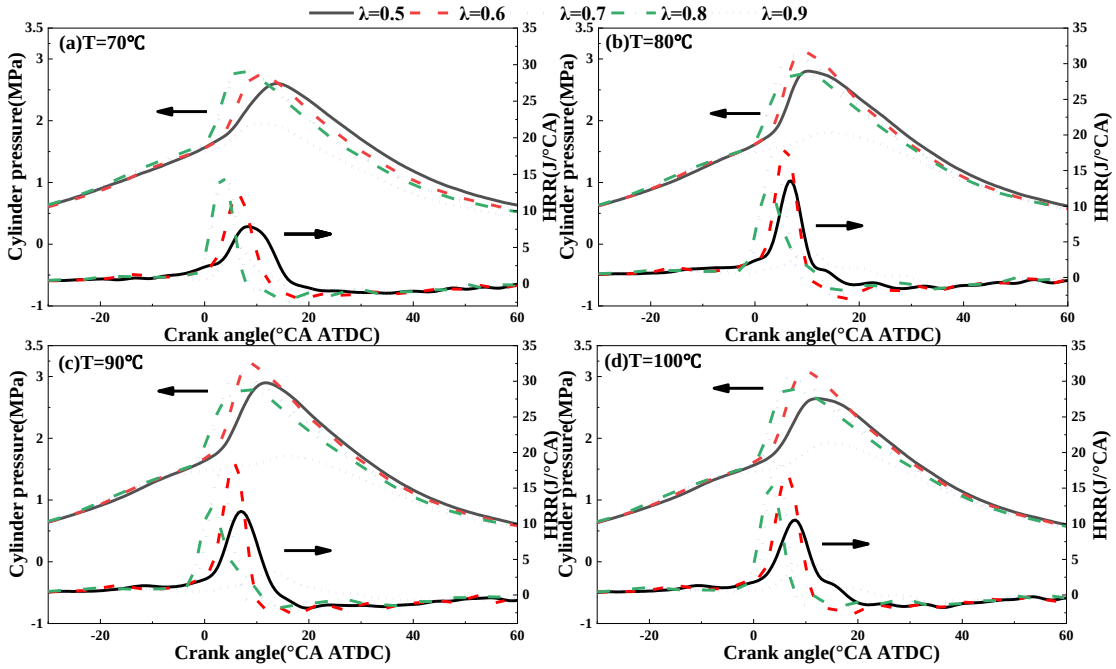

Fig. 3. Cylinder pressure and *HRR* under various λ with *T* =70 ℃ (a), *T* =80 ℃ (b), *T*=90 ℃ (c), and *T* =100 ℃ (d).

3.1.2 Peak in-cylinder temperature

The peak in-cylinder temperature (T_{max}) is one of the key parameters for characterizing the combustion process. Fig. 4 illustrates the variation of T_{max} under different λ and T. At T=70 °C, T_{max} increases as λ decreases. With the T further increase to 80 ℃, T_{max} rises rapidly. This indicates that as T increases within this range. It has a significantly positive effect on heat release during combustion, with the maximum value of T_{max} occurring at λ=0.6. From Fig. 3(b), the combustion rate is faster, and the heat release is more concentrated at this λ. This results in reduced heat loss during the expansion work phase, which contributes to an increase in T_{max}. However, the change of T_{max} becomes less pronounced when T continues to rise. This indicates that while further increasing T may positively affect fuel atomization characteristics, and it could also lead to a deterioration of intake flow characteristics. This dual effect diminishes the enhancement of combustion reaction rates by T, resulting in a reduced increase in T_{max}.

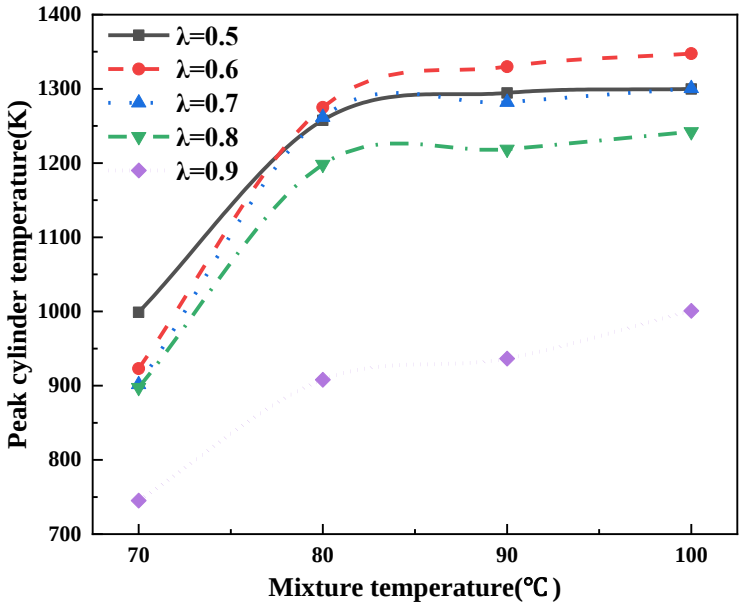

Fig. 4. The peak in-cylinder temperature under different λ and T.

3.1.3 Combustion parameter

θ_{ID} reflects the time required for heating, evaporation, diffusion, mixing, and other physical and chemical preparatory processes of the fuel, which is significantly impacting engine combustion performance. Fig. 5 illustrates the variation of θ_{ID} under different λ and T. It shows that θ_{ID} gradually increases with λ decreases. A smaller λ indicates that more time is required for evaporating atomization during the initial combustion stage to achieve ignition concentration. When T=70-80 °C, θ_{ID} shows little variation, with a maximum difference of only 0.5 °CA. As the mixture temperature increases further, θ_{ID} shows a trend of first decreasing and then increasing, with the minimum value observed at T=90 °C. This is understood to mean that when T rises it directly affects the quality of the air entering the cylinder, mainly including characteristics such as density, temperature, and oxygen content.

When T=70-80 ℃, these characteristics decrease but still maintain optimal conditions for aviation kerosene evaporation, preventing the process from becoming either too rapid or too slow. As a result, there is minimal variation in the ignition delay. When T=90 ℃, these characteristics continue to decline, potentially maintaining the optimal mixture formation rate and resulting in the shortest ignition delay. When T=100 ℃, the fuel evaporation rate increases. However, the air mass mixed with the fuel becomes progressively thinner, leading to the formation of localized dense regions, which complicate ignition. Consequently, the ignition delay increases significantly.

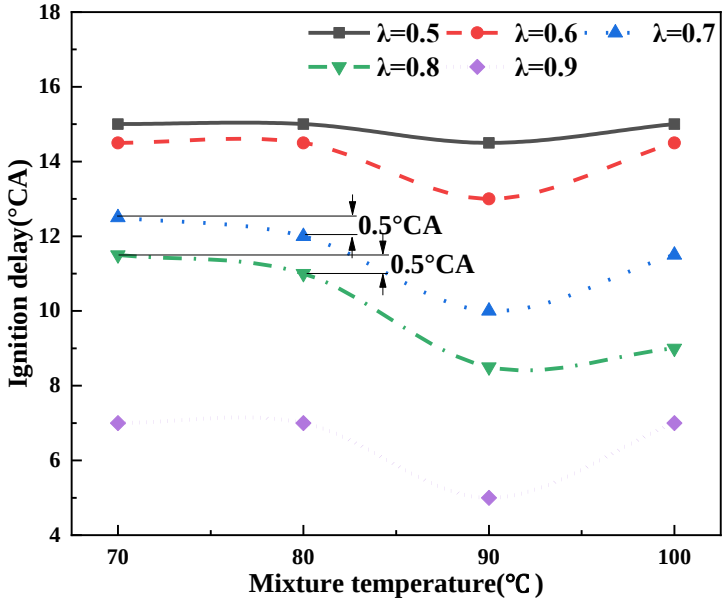

Fig. 5. θ_{ID} under different λ and T.

θ_{CC} is one of the key indicators for assessing the combustion phase. Fig. 6 illustrates the variation of θ_{CC} under different λ and T. It shows that θ_{CC} initially advances before experiencing a delay as λ increases. Because a larger λ means more air and less fuel within the same volume. A higher proportion of oxygen accelerates the initial flame development, resulting in the advancement of θ_{CC}. However, as λ increases further, the flame propagation can become unstable, leading to a subsequent delay in θ_{CC}. In the range of λ=0.6-0.8, θ_{CC} initially advances and then delays as T increases. It promotes combustion reactions between fuel and oxygen molecules, which is accelerating the flame propagation process and advancing θ_{CC}. However, when T>90 °C, insufficient oxygen supply in the cylinder slows combustion speed, which is causing θ_{CC} to delay. When λ=0.9, θ_{CC} delays when T increases. This phenomenon occurs due to a reduction in both fuel molecules and fresh charge entering the cylinder. This results in slower flame propagation and increased instability during the combustion process. Although rising T enhances the likelihood of chemical reactions, it may not sufficiently counter balance the negative effects of reduced oxygen content.

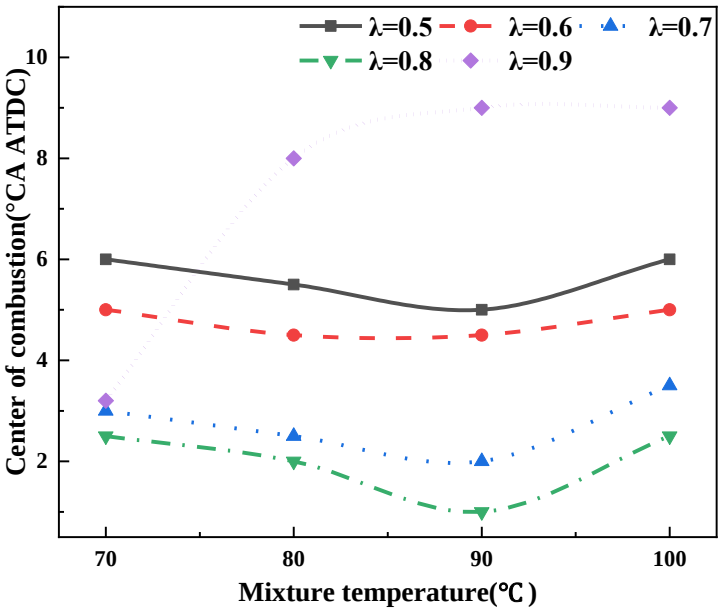

Fig. 6. θ_{CC} under different λ and T.

θ_{CD} indicates the speed and efficiency of fuel combustion. Fig. 7 illustrates the variation of θ_{CD} under different λ and T. The θ_{CD} first decreases and then increases as λ increases. This occurs because a lower fuel-to-air ratio accelerates the reaction in the initial combustion stage, as evidenced in Fig 6. As the mixture becomes leaner, the decrease in fuel molecules hinders the continuation of combustion reactions, gradually slowing the flame propagation speed. At λ=0.9, flame propagation slows significantly. This instability results in an extended trailing off of the *HRR* curve, causing an increase in combustion duration. When λ=0.5-0.8, θ_{CD} reaches a minimum at T=80 °C. Fig 6 indicates that the center of combustion minimum becomes more concentrated at T=90 °C. Therefore, appropriately lowering T to enhance intake air flow can facilitate faster flame propagation in the latter half of the combustion process.

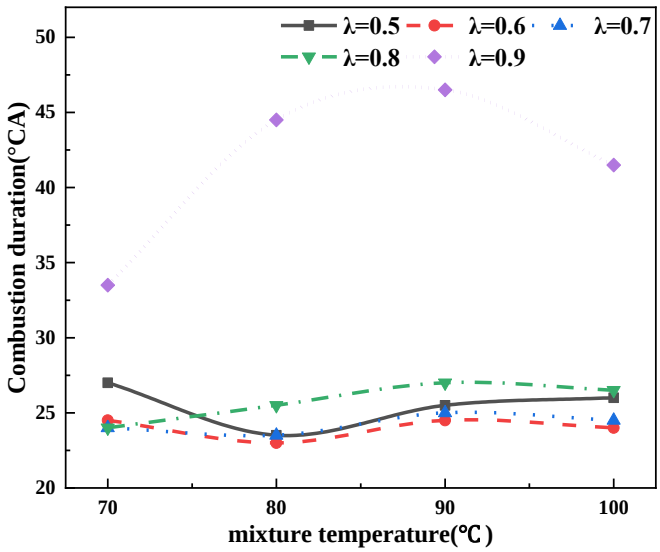

Fig. 7. θ_{CD} under different λ and T.

3.2. Engine performance

3.2.1 Brake power

Brake power is one of the key indicators for assessing the overall performance of the engine. Fig. 8 illustrates the variation of power under different λ and T. It reveals that power initially increases and then decreases when λ and T increases. When λ=0.6, the highest power output is observed under all temperature conditions, with the maximum value approaching 1.5 kW. When T=70-80 ℃, power output is significantly affected. The increasing the temperature within this range leads to better improvement in fuel atomization. This results in a more uniform mixture distribution and enhances combustion efficiency. However, when T=100 °C, the combustion rate is reduced due to a decrease in the air-fuel ratio. Excessively high temperatures may increase the likelihood of knocking. The decline in power output is observed. The analysis indicates that λ=0.6 and T=80 °C represent the optimal power conditions during the start-up phase discussed in this paper.

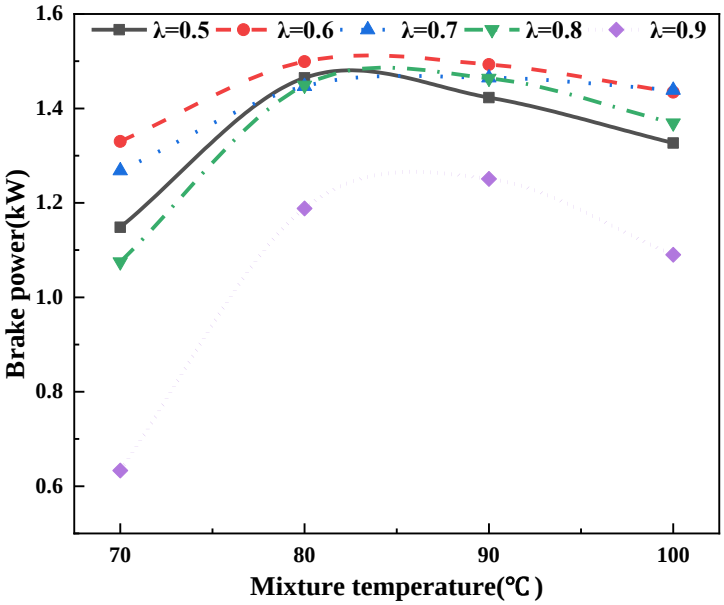

Fig. 8. Brake power under different λ and T.

3.2.2 Misfire rate

In this paper, the cycle greater than 130% of the compression peak pressure is defined as the combustion cycle. Otherwise, it is classified as a misfire cycle [30]. Fig. 9 illustrates the variation of misfire rate under different λ and T. The engine misfire rate initially decreases and then increases when λ decreases. When λ=0.5-0.8, the misfire rate gradually decreases with increasing of T. At λ=0.5, the engine misfire rate decreases from over 40% initially to less than 10%. This indicates that the probability of misfire is significantly reduced by the increase of T. At λ=0.6, the lowest misfire rate is achieved across various T conditions, and increasing temperature proves effective in reducing the misfire rate. Conversely, the overall misfire rate is significantly higher than at other λ values at λ=0.9. As T increases, the misfire rate initially rises and then decreases. In the case of a dilute mixture, the slower combustion

reaction rate increases the likelihood of incomplete combustion or combustion instability. It leads to a higher misfire rate. Reducing the amount of air intake during this phase facilitates the formation of a more homogeneous mixture in the engine.

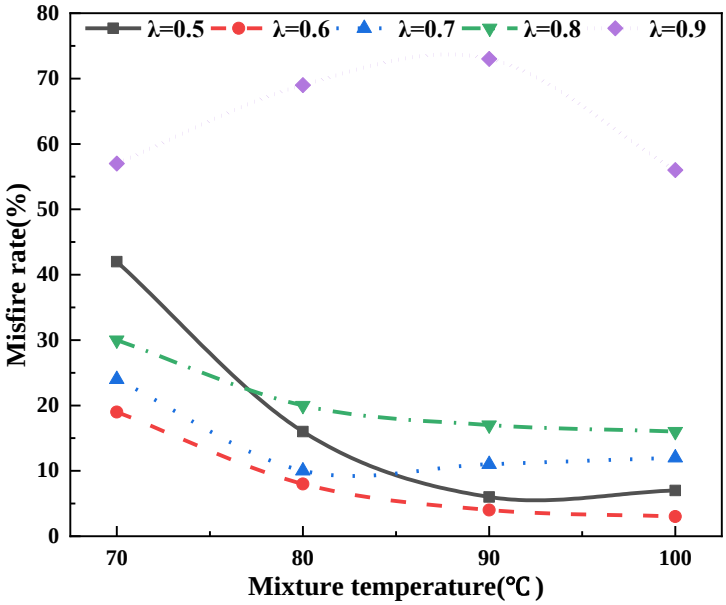

Fig. 9. Misfire rate under different λ and T.

3.2.3 Cyclic variations

COV_{IMEP} reflects the degree of variation in the continuous engine cycle. Fig. 10 illustrates the variation of COV_{IMEP} under different λ and T. The COV_{IMEP} exhibits a characteristic trend of first decreasing and then increasing as λ increases. At λ=0.6, the COV_{IMEP} reaches its minimum value across all temperature conditions. The combustion process is more stable. When λ=0.5-0.6, as the T increases, the reduction in COV_{IMEP} approaches half of its initial value. When λ=0.7-0.9, further increases in T=70-80 °C also substantially improve COV_{IMEP}. However, as T continues to rise, the COV_{IMEP} curve fluctuates within 5%. This indicates that the effect of temperature on COV_{IMEP} exhibits non-ideal development. These observations show that the interaction between λ and T creates an optimal operating window for enhancing combustion stability during the engine start-up phase. Adjustments made within this window are beneficial for improving COV_{IMEP}. Whereas adjustments outside this range may not only fail to provide benefits but could also worsen the combustion conditions.

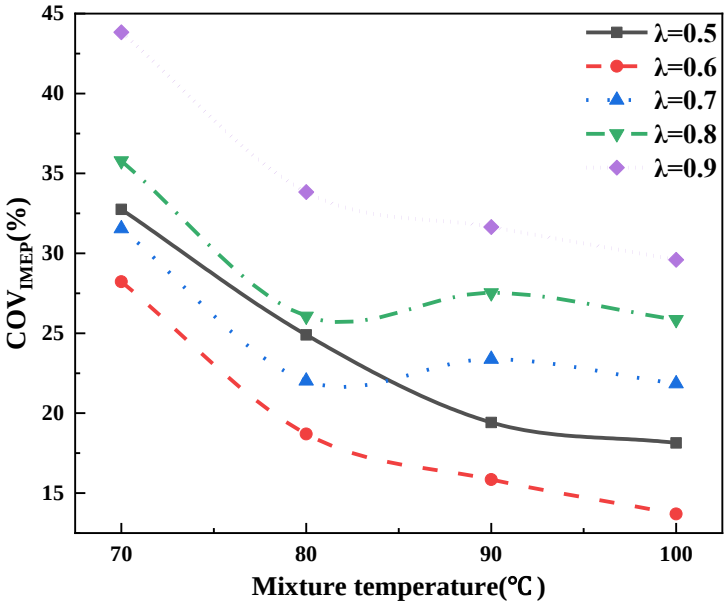

Fig. 10. COV_{IMEP} under different λ and T.

3.3. Multiple linear regression analysis

In the engine start-up stage, the misfire rate and COV_{IMEP} are important indicators directly related to the engine's ability to start normally. There is a strong correlation between them and the ignition characteristics. By analyzing the degree of correlation between these parameters, it becomes possible to identify the ignition characteristics most sensitive to both the misfire rate and COV_{IMEP}. This can help develop more effective control strategies. In this paper, the primary influencing factors for the engine misfire rate and COV_{IMEP} are identified as θ_{ID}, θ_{CD}, and T_{max}. Results obtained through linear regression analysis, represented by Eqs. (5)-(8). Their corresponding R-squared values are 0.949, 0.502, 0.873, and 0.893, respectively, which indicate the models have strong explanatory power and the data is available. The analysis results indicate that the misfire ratio is most sensitive to θ_{CD}, showing a positive correlation. In contrast, its sensitivity to θ_{ID} and T_{max} is lower and exhibits a negative correlation. The sensitivity of COV_{IMEP} to θ_{ID}, θ_{CD}, and T_{max} decreases in that order, which is maintaining a negative correlation with all three. Additionally, θ_{ID} and θ_{CD} are highly sensitive to λ but show weak sensitivity to T.

$$Misfire\ ratio = 30.282 - 0.128\theta_{ID} + 1.964\theta_{CD} - 0.052T_{\max} \quad (5)$$

$$\theta_{CD} = -1.995 + 33.75\lambda + 0.077T \quad (6)$$

$$COV_{IMEP} = 82.099 - 0.805\theta_{ID} - 0.268\theta_{CD} - 0.035T_{\max} \quad (7)$$

$$\theta_{ID} = -29.243 - 20.875\lambda - 0.038T \quad (8)$$

4. Conclusion

In this paper, the two-stroke SI engine is investigated, which is focusing on the ignition characteristics and performance during its start-up stage. Furthermore, the influence weight relationships among these parameters are established. The following conclusions are drawn:

1. Both P_{max} and HRR_{max} exhibit an initial increase followed by a decrease with variations in λ and T. T_{max} increases significantly in the T=70-80 °C range. θ_{ID} decreases as λ increases, with its minimum value consistently occurring at T=90 °C. θ_{CC} and θ_{CD} display more complex responses to changes in λ and T. This indicates that under specific conditions, improved combustion phases and faster combustion speeds can be achieved.

2. When λ=0.6 and T=80-90 °C, optimal output power can be achieved, along with reduced misfire rates and cyclic variation.

3. The sensitivity of Misfire rate to θ_{CD}, θ_{ID} and T_{max} decreased successively. The sensitivity to θ_{ID}, θ_{CD} and T_{max} decreases sequentially. The influence of λ on θ_{CD} and θ_{ID} is particularly obvious.

This study adopts a port fuel injection two-stroke engine. Due to scavenging losses, the actual amount of fuel and intake air participating in combustion within the cylinder cannot be accurately measured. This leads to an incomplete analysis of combustion parameters. Further development of an engine intake and exhaust model is needed to explore the scavenging process in depth.

Acknowledgment

This work was sponsored by the National Defense Science and Technology Key Laboratory Fund Project (grant number 2022-JCJQ-LB-062-0102), the Sichuan Science and Technology Program (grant number 2023NSFSC0836), the Open Research Subject of Key Laboratory of Fluid Machinery and Engineering (Xihua University), Sichuan Province (grant number LTJX-2024005), and the Chunhui Plan of the Ministry of Education of the People's Republic of China (grant numbers HZKY20220586, HZKY20220569).

Nomenclature

ATDC	– After the top dead center
BTDC	– Before the top dead center
COV_{IMEP}	– Cyclic variations
ECU	– Electronic control unit
HRR	– The heat release rate
HRR_{max}	– The peak of HRR
IMEP	– Indicated mean effective pressure
n	– Engine speed
P_{max}	– The peak cylinder pressure
SI	– Spark ignition
T	– Mixture temperature
T_{max}	– The peak in-cylinder temperature
TP	– Throttle opening
UAVs	– Unmanned Aerial Vehicles
λ	– Mixture concentration
θ_{CC}	– Crank angle degree at which 50% accumulative heat released
θ_{CD}	– Crank angle degree at which 90% accumulative heat released

θ_{ID} – Crank angle degree at which 10% accumulative heat released
°CA – Crank angle degree

References

[1] Newcome, L.R., Unmanned aviation: A brief history of unmanned aerial vehicles, AIAA, Reston, USA, 2004

[2] Hayat S., et al., Survey on unmanned aerial vehicle networks for civil applications: A communications viewpoint, *IEEE Communications Surveys & Tutorials*, *18*(2016), 4, pp. 2624–2661

[3] Zhou, G., et al., Foreword to the Special Issue on Unmanned Airborne Vehicle (UAV) Sensing Systems for Earth Observations. *IEEE Transactions on Geoscience and Remote Sensing*. *47*(2009), 3, pp. 687–689

[4] Nex F., Remondino F., UAV for 3D mapping applications: A review, *Appl Geomat*, *6*(2014), pp. 1–15

[5] Pickett, B. M. et al., Fire safety tests comparing synthetic jet and diesel fuels with JP-8, *The Lancet*, *46*(2010), 3, pp. 89-95

[6] Falkowski, D., et al., The performance of a spark-ignited stratified-charge two stroke engine operating on a kerosine based aviation fuel, *SAE Transactions, 106*(1997), pp. 2169–2177

[7] Le N., et al., Effects of injection timing and compression ratio on the combustion performance and emissions of a two-stroke DISI engine fueled with aviation kerosene, *Applied Thermal Engineering*, *161*(2019), pp. 114-124

[8] Liu R., et al., Combustion characteristics of a two-stroke spark ignition UAV engine fueled with gasoline and kerosene (RP-3), *Aircraft Engineering and Aerospace Technology, 91*(2019), 1, pp. 163-170

[9] Zhao Z., Cui H., Numerical investigation on combustion processes of an aircraft piston engine fueled with aviation kerosene and gasoline, *Energy, 239*(2022), 122264

[10] Suhy P., et al., The feasibility of a kerosene fueled spark ignited two-stroke engine, International Off-Highway & Powerplant Congress and Exposition, Milwaukee, USA, 1991

[11] Zhou Y., et al., Technologies and studies of gas exchange in two-stroke aircraft piston engine: A review, *Chinese Journal of Aeronautics, 37*(2024), 1, pp. 24-50.

[12] Wang L., et al., Experimental study of aviation kerosene engine with PJI system, *Energy, 248*(2022), 123590

[13] Hooper P., Experimental experience of cold starting a spark ignition UAV engine using low volatility fuel, *Aircraft Engineering and Aerospace Technology, 89*(2017), 1, pp. 106-111

[14] Elliott L., et al., Genetic algorithms for optimisation of chemical kinetics reaction mechanisms, *Progress in Energy and Combustion Science, 30*(2004), 30, pp. 297-328

[15] Yu B., et al., Development of a Chemical-Kinetic Mechanism of a Four-Component Surrogate Fuel for RP-3 Kerosene, *ACS Omega, 6*(2021), 36, pp. 23485-23494

[16] Mao Y., et al., Experimental and kinetic modeling study of ignition characteristics of RP-3 kerosene over low-to-high temperature ranges in a heated rapid compression machine and a heated shock tube, *Combustion and Flame, 203*(2019), pp. 157-169

[17] Yang Z., et al., Ignition characteristics of an alternative kerosene from direct coal liquefaction and its blends with conventional RP-3 jet fuel, *Fuel, 291*(2021), 120258

[18] Meng K., et al., Experimental investigation on ignition, combustion and micro-explosion of RP-3, biodiesel and ethanol blended droplets, *Fuel, 178*(2020), 115649

[19] Liu J., et al., A new surrogate fuel for emulating the physical and chemical properties of RP-3 kerosene, *Fuel, 259*(2020), 116210

[20] Wang C., et al., Explosion behaviors of aviation kerosene in a 20-L spherical vessel, *Aerospace Science and Technology, 152*(2024), 109308

[21] Chen Z., et al., Effect of equivalence ratio on spark ignition combustion of an air-assisted direct injection heavy-fuel two-stroke engine, *Fuel, 313*(2022), 122646

[22] Wei D., et al., Ignition and combustion characteristics of wall-impinged kerosene (RP-3) fuel spray with varying injection parameters, *Thermal Science*, 24(2020), pp. 171-181

[23] Chang C., et al., Experimental Research on Cold Start of PFI Two-Stroke Spark-Ignition Kerosene Engine, *Journal of Energy Engineering, 146*(2020), 04020030

[24] Li S., et al., Study on the ignition factor of piston kerosene engine, *Advanced Materials Research, 779*(2013), pp. 705-710

[25] Zhang S., et al., Orthogonal experimental study on the cold-start control strategies of a SI aviation piston engine fueled with kerosene, *Fuel, 328*(2022), 124880

[26] Liang J., et al., The vitiation effects of water vapor and carbon dioxide on the autoignition characteristics of kerosene, *Acta Mechanica Sinica, 30*(2014), 4, pp. 485-494

[27] Javed I., et al., Autoignition and combustion characteristics of kerosene droplets with dilute concentrations of aluminum nanoparticles at elevated temperatures, *Combustion and Flame, 162*(2015), 3, pp. 774-787

[28] Javed I., et al., Evaporation characteristics of kerosene droplets with dilute concentrations of ligand-protected aluminum nanoparticles at elevated temperatures, *Combustion and Flame, 160*(2013), pp. 2955-2963

[29] Heywood J.B., Internal combustion engine fundamentals, New York, USA, 1988

[30] Chang C., et al., Experimental Research on Cold Start of PFI Two-Stroke Spark-Ignition Kerosene Engine, *Journal of Energy Engineering, 146*(2020), 04020030

Paper submitted: 27.10.2024

Paper revised: 27.12.2024

Paper accepted: 02.01.2025